Molecular Catalysis 442 (2017) 181–190

Contents lists available at ScienceDirect

Molecular Catalysis

journal homepage: www.elsevier.com/locate/mcat

MCAT

Editor's choice paper

Double-active sites cooperatively catalyzed transfer hydrogenation of ethyl levulinate over a ruthenium-based catalyst

Zhi Gao, Guoli Fan*, Lan Yang, Feng Li*

State Key Laboratory of Chemical Resource Engineering, Beijing Advanced Innovation Center for Soft Matter Science and Engineering, Beijing University of Chemical Technology, Beijing, 100029, China

ARTICLE INFO

Article history:
Received 17 July 2017
Received in revised form 4 September 2017
Accepted 23 September 2017

Keywords:
Ruthenium
Double-active sites
Cooperative effect
Catalytic transfer hydrogenation
Ethyl levulinate

ABSTRACT

Presently, designing high-performance catalyst systems for the sustainable production of chemicals through biomass conversions is of significant importance for large-scale practical application. As for heterogeneous catalysts, the high dispersion of active species can play a vital role in guaranteeing their superior performance. In this regard, the combination of active species with a favorable support matrix is crucial for achieving highly dispersive character of active species and the formation of cooperation between them. Herein, we first synthesized a novel ruthenium-based catalyst, Ru/Zn-Al-Zr layered double hydroxide (Ru/ZnAlZr-LDH), which was employed in the transfer hydrogenation of biomass-derived ethyl levulinate (EL) into γ-valerolactone (GVL) using 2-propanol as hydrogen donor. Extensive characterizations revealed that the interaction between Ru species and the ZnAlZr-LDH matrix helped enhance the dispersion of Ru species on the LDH and also determined the nature of electron-rich Ru species. Furthermore, a cooperative effect between double-active sites on the catalyst, e.g. a large amount of surface hydroxyl groups and highly dispersive electron-rich Ru species, was beneficial to the formation of both activated six-membered ring transition state and active ruthenium-hydride species in the course of EL transfer hydrogenation, thereby resulting in an unparalleled activity with a fastest GVL formation rate of 1250 μmol g_{cat}^{-1} min^{-1} to date, with respect to other Zr- or Ru-based catalysts previously reported.

1. Introduction

Currently, with the rapid development of economy and human society, the consumption of non-renewable fossil resources is increasing year by year. Meanwhile, the use of fossil resources also brings out serious environmental pollution problems and global climate change. Correspondingly, exploring a wide range of new, safe, environmentally friendly and sustainable resources and energy sources is of significant importance. As an ideal alternative to fossil resources, abundant renewable raw biomass especially can be converted into various liquid transportation fuels and valuable chemicals [1–3]. For example, cellulose may be transformed into many kinds of desired platform molecules [4–10]. Among them, levulinic acid is regarded as one of the most important biomass-derived platform compounds due to its excellent reactive nature. Specially, hydrogenating levulinic acid or its esters can generate another important platform molecule, γ-valerolactone (GVL) [11–15], which is identified as a key sustainable biomass conversion. GVL may be widely transformed into various important chemicals [16], such as suitable reaction solvents for biomass upgrading [17–19], excellent food and fuel additives [20,21], and liquid fuel precursors [22–24].

Due to easy deactivation and low stability of precious metal catalysts, strong acidity and low volatility of levulinic acid, and need of high hydrogen pressure, large-scale production of GVL through the hydrogenation of levulinic acid is limited. Comparably, hydrogenating ethyl levulinate (EL) to produce GVL is regarded as an economical and eco-friendly alternative, because high yields of EL can be directly achieved through ethanolysis of lignocellulose biomass and GVL product is more easily separated and purified [25,26]. Meanwhile, considering many drawbacks of external molecular hydrogen obtained from non-renewable substances, such as low utilization, poor security, and difficulty in storage and transportation, using formic acid as hydrogen source for the production of GVL has been investigated [27,28]. In spite of high GVL yields, the corrosive nature of formic acid, as well as harsh reaction conditions, limits its practical application. Therefore, exploring suitable hydrogen donors for the production of GVL is highly desirable.

In recent years, non-corrosive alcohols have been utilized as both hydrogen donors and solvents in the transfer hydrogenation

* Corresponding author.
E-mail addresses: fangl@mail.buct.edu.cn (G. Fan), lifeng@mail.buct.edu.cn (F. Li).

http://dx.doi.org/10.1016/j.mcat.2017.09.026
2468-8231/

of EL to produce GVL [29–34], considering the fact that alcohols can be produced from renewable biomass resources and dehydrogenated aldehydes or ketones formed are valuable chemicals. In this regard, different Zr-based catalysts (e.g., Zr-Beta zeolite [29], metal hydroxides [30,31], ZrO_2 [32], Zr-containing catalyst with a phenate [33]) exhibit good catalytic performance in the EL transfer hydrogenation using alcohols as hydrogen donors, mostly via Meerwein–Ponndorf–Verley (MPV) reduction pathway. Despite many efforts, in most cases, current catalytic systems often require long reaction time, large amounts of catalysts, or high pressure of inert gas, in order to facilitate the dehydrogenation of alcohols and promote the reaction equilibrium, thus leading to high energy consumption and even catalyst leaching. As for transfer hydrogenation of EL, the present limited design strategy of heterogeneous catalysts hinders the rational improvement of their catalytic performances.

Thanks to the versatility and flexibility of microstructures and compositions, layered double hydroxides (LDHs, $[M_{1-x}^{2+}M_x^{3+}(OH)_2]^{x+}A_{x/n}^{n-}\cdot mH_2O$), well known as a class of highly ordered two-dimensional layered clay materials, have been widely used as catalyst supports in various heterogeneous catalytic processes [35–37]. Especially, it was reported that regular hydroxyl arrays on positively charged two-dimensional brucite-like sheets of LDHs as Brønsted base sites could promote the MPV reactions of aldehydes with alcohols [30,38], as well as other organic reactions including condensation [39,40], transesterification [41], and isomerization [42].

Herein, we first synthesized a new ruthenium-based catalyst (Ru/ZnAlZr-LDH) and reported its unparalleled activity in the EL transfer hydrogenation to produce GVL and mechanistic understanding of the promotion effect. An extensive investigation indicated that the immobilization of Ru species on the ZnAlZr-LDH matrix could induce the formation of highly dispersed electron-rich Ru species due to the strong interaction between Ru species and surface hydroxyl groups of ZnAlZr-LDH, and the resulting catalyst gave a GVL yield of 98% only within 10 min, along with a fastest GVL formation rate of 1250 $\mu mol\, g_{cat}^{-1}\, min^{-1}$ to date, with respect to other Zr- or Ru-based catalysts previously reported. The activity of the catalyst was higher than those exhibited by bare ZnAl-LDH, Zr substituted ZnAl-LDH, and ZnAl-LDH supported Ru catalyst. Such unprecedented catalytic performance of Ru/ZnAlZr-LDH was ascribed to a cooperative effect between double-active sites on the catalyst, e.g. a large amount of surface hydroxyl groups of the ZnAlZr-LDH and highly dispersive electron-rich Ru species, which was beneficial to the formation of both activated six-membered ring transition state and active ruthenium-hydride species in the course of transfer hydrogenation, thereby greatly improving the dehydrogenation of isopropanol and the hydrogenation of EL. Moreover, the activity of as-synthesized ruthenium-based heterogeneous catalyst kept almost unchanged after it was reused more than six times. Until now, this is the first report about the application of such highly efficient LDH supported Ru catalyst for the transfer hydrogenation of EL to produce GVL.

2. Experimental

2.1. Synthesis of catalysts

Ru/ZnAlZr-LDH sample was synthesized through a separate nucleation and aging steps method previously developed by our group [43]. In a typical experiment, first, $RuCl_3\cdot 3H_2O$, $Zn(NO_3)_2\cdot 6H_2O$, $Al(NO_3)_3\cdot 9H_2O$ and $Zr(NO_3)_4\cdot 5H_2O$ with a Ru/Zn/Al/Zr molar ratio of 1.5:75:15:10 were dissolved in 100 mL deionized water to obtain a salt solution, while Na_2CO_3 and NaOH ($[CO_3^{2-}] = 2([Al^{3+}] + [Ru^{3+}] + [Zr^{4+}])$; $[OH^-] = 1.6([Zn^{2+}] + [Al^{3+}] + [Ru^{3+}] + [Zr^{4+}])$) were also dissolved in 100 mL deionized water to form a mixed base solution. Then, above salt and base solutions were simultaneously added to a colloid mill, rapidly mixed at a rotor speed of 3000 rpm for 2 min. The resulting suspension was centrifuged and washed with deionized water until pH value reaches 7.0, and then dried at 70 °C overnight.

For comparison, pure M_1Al-LDH (M_1 = Zn, Mg, Ni, or Co; M_1/Al molar ratio = 75:25), pure ZnAlZr-LDH (Zn/Al/Zr molar ratio = 75:15:10), Ru/ZnAl-LDH (Ru/Zn/Al molar ratio = 1.5:75:25), M_2/ZnAlM_3-LDH (M_2 = Ru, Au, or Pd; M_3 = Zr or Sn; M_2/Zn/Al/M_3 molar ratio = 1.5:75:15:10) samples also were synthesized according to the same procedure as for Ru/ZnAlZr-LDH. In addition, $Zr(OH)_4$ supported Ru catalyst with the Ru loading of about 0.9 wt%, $Ru(OH)_3/Zr(OH)_4$, was prepared by incipient wetness impregnation using the $Zr(OH)_4$ support. And, metallic Ru^0 also was loaded on the ZnAlZr-LDH to obtain Ru^0/ZnAlZr-LDH sample with the Ru loading of 0.9 wt.%. First, ZnAlZr-LDH powder (0.5 g) was added into 100 mL of $RuCl_3\cdot 3H_2O$ aqueous solution (10 mM). Then, the obtained suspension was stirred at room temperature for 2 h. Subsequently, 17 mL of $NaBH_4$ solution (0.16 M) was added into the above suspension under ice water bath and maintained for 6 h under nitrogen atmosphere. Finally, Ru^0/ZnAlZr-LDH obtained was centrifuged, washed with deionized water and dried at 70 °C overnight under vacuum.

2.2. Characterization

X-ray diffraction (XRD) patterns of samples were recorded at room temperature using Shimadzu XRD-6000 diffractmeter with graphite-filtered Cu Kα source (λ = 0.15418 nm) at a scanning rate of 10°/min, and 2θ angle ranging from 3° to 70°.

Elemental analysis of samples was carried out on a Shimadzu ICPS-7500 inductively coupled plasma atomic emission spectroscope (ICP-AES). The samples were dissolved in nitrohydrochloric acid before measurements.

N_2 adsorption-desorption isotherms of samples were obtained on a Micromeritics ASAP 2020 sorptometer apparatus at −196 °C. The total specific surface areas were determined by the multipoint Brunauer-Emmett-Teller (BET) method.

High-resolution transmission electron microscopy (HRTEM) were measured using a JEOL 2100 operated at an accelerating voltage of 200 kV. High-angle annular dark-field scanning transmission electron microscopy with energy-dispersive X-ray spectroscopy (HAADF-STEM-EDX) measurements of the sample was investigated using a JEOL2010F instrument.

X-ray photoelectron spectroscopy (XPS) measurements were performed using a VG ESCALAB 2201 XL spectrometer with monochromatic Al Kα X-ray radiation (1486.6 eV photons). The binding energy calibration of all spectra was referenced to the C 1s signal at 284.6 eV.

The number of basic sites was obtained using a method based on the irreversible adsorption of organic acids with different pK_a values, e.g. acrylic acid (pK_a = 4.2) and phenol (pK_a = 9.9) [44,45].

In situ Fourier transform infrared (FT-IR) spectra of EL or pyridine adsorption were recorded using a Thermo Nicolet 380 FT-IR spectrometer. The sample (30 mg) pressed into a self-supporting wafer was placed into an evacuable IR cell with CaF_2 windows, and then evacuated at 100 °C for 1 h. After cooling to 30 °C, EL or pyridine was introduced and held for 1 h. Finally, physically adsorbed EL or pyridine was removed by evacuation under vacuum.

2.3. Catalytic transfer hydrogenation of EL

The liquid phase transfer hydrogenation of EL was performed in a 100 mL stainless steel autoclave under magnetic stirring. In a typical experiment, EL (2.8 mmol), isopropanol (131 mmol) and the catalyst (0.1 g) were charged into the reactor. Before each run,

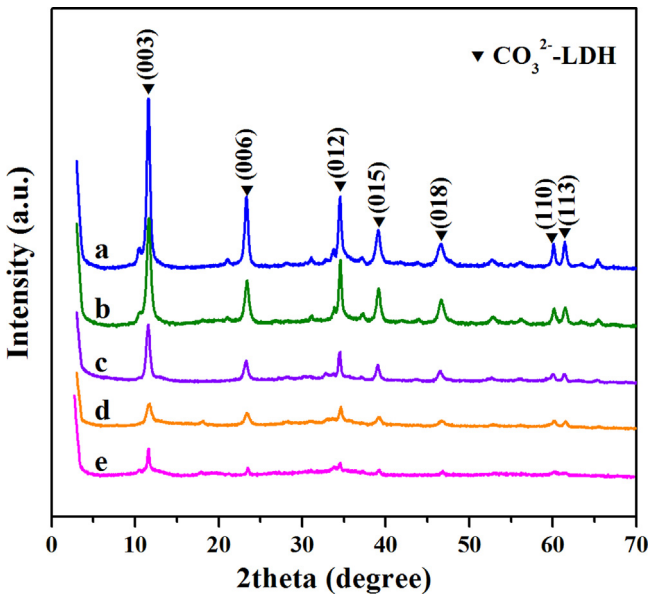

Fig. 1. XRD patterns of (a) ZnAl-LDH, (b) Ru/ZnAl-LDH, (c) ZnAlZr-LDH, (d) Ru/ZnAlZr-LDH and (e) Ru/ZnAlSn-LDH.

the reactor was sealed and flushed with 2 MPa N_2 for ten times to remove the air. Then, the reactor was initiated by stirring with a rate of 900 rpm at a designated temperature under N_2 atmosphere. After reaction, the autoclave was cooled to room temperature and depressurized carefully. The reaction products were filtered to obtain a clear solution and then analyzed using Agilent GC7890 B gas chromatograph equipped with a flame ionization detector and a DB-wax capillary column (30.0 m × 250 μm × 0.25 μm). The products were identified by comparison with known standards, and toluene was used as an internal standard to quantitatively analyze liquid products with a standard deviation less than 2%. In each case, the mass balance was above 97%.

3. Results and discussion

3.1. Structural characterization

Fig. 1 illustrates the XRD patterns of ZnAl-LDH, Ru/ZnAl-LDH, ZnAlZr-LDH, Ru/ZnAlZr-LDH and Ru/ZnAlSn-LDH samples. In all cases, typical characteristic diffractions indexed to (003), (006), (012), (015), (018), (110) and (113) planes of carbonate-type hydrotalcite-like materials can be found, indicating the successful synthesis of LDH materials [46,47]. Compared with ZnAl-LDH sample, other samples present relatively weakened intensities of diffractions, indicating that the introduction of Ru, Zr or Sn leads to the decreased crystallinity of LDH phases, as well as the formation of small LDH particle with reduced size. No characteristic diffractions assignable to metallic Ru and RuO_2 phases are observed in Ru-containing samples, suggesting that Ru species should be highly dispersed on the surface of LDHs or exist in bulk phase in the form of other chemical states. Further, typical HRTEM images of the representative Ru/ZnAlZr-LDH sample clearly depict that the sample has the sheet-like feature of LDH materials (Fig. 2a, b). No aggregates of small particles possibly related to Ru species can be observed. HAADF-STEM-EDX images (Fig. 2c, d) reveal the uniform surface distributions of Zn, Al, Zr and Ru elements, indicative of highly dispersive nature of these elements on the sample. In addition, as for Ru-containing samples, the Ru loadings confirmed by ICP-AES are about 0.9 wt%, in good accordance with the theoretical values. Moreover, Table 1 shows that the BET specific surface area of Ru/ZnAlZr-LDH (119 m^2/g) is higher than other samples (42 m^2/g for ZnAl-LDH, 57 m^2/g for Ru/ZnAl-LDH and 93 m^2/g for ZnAlZr-LDH). As evidenced in Fig. 1, Ru/ZnAlZr-LDH and Ru/ZnAl-LDH samples present relatively weakened diffraction intensities compared with ZnAlZr-LDH and ZnAl-LDH sample, respectively. It demonstrates that the introduction of Ru leads to the decreased crystallinity of LDH phases, as well as the formation of LDH crystals with the reduced particle size. Therefore, a smaller particle size of Ru/ZnAlZr-LDH than ZnAlZr-LDH can give rise to a higher specific surface area of Ru/ZnAlZr-LDH sample.

3.2. Catalytic performance of catalysts

Preliminary, we examined the EL transfer hydrogenation over different pure base LDH supports with various binary metal cations. The catalytic results are presented in Table 2. Obviously, the EL transfer hydrogenation using isopropanol as hydrogen source can perform over the ZnAl-LDH support; it affords an EL conversion of 24% with a GVL selectivity of 65% after reaction for 30 min at 200 °C (entry 1). The major by-product is isopropyl levulinate formed through the transesterification of EL with isopropanol. Noticeably, other LDH supports of MgAl-LDH, NiAl-LDH and CoAl-LDH exhibit much less catalytic activity for the reaction (entries 2–4). Among them, remarkably, ZnAl-LDH support shows the best activity.

Further, the catalytic performances of various Zr and/or Ru-containing catalysts for the EL transfer hydrogenation were tested. When Zr is introduced into the lattice of brucite-like layers, an improved yield of GVL by 20% can be achieved over the ZnAlZr-LDH (entry 5). In the presence of Ru/ZnAl-LDH, the EL conversion and the GVL selectivity sharply increase to 78% and 90% (entry 6), respectively, indicating a promotional effect of the introduction of Ru into the catalyst on the EL transfer hydrogenation. Compared with Ru/ZnAl-LDH, Ru/ZnAlZr-LDH sample with the same Ru load-

Table 1
Textural properties and surface basicity of different samples.

Samples	S_{BET}[a] (m^2/g)	V_p[b] (cm^3/g)	d_p[c] (nm)	Total base sites (mmol acrylic acid/g)	Distribution of base sites	
					Medium-strength and strong base sites (mmol phenol/g)	Weak base sites[d] (mmol/g)
ZnAl-LDH	42	0.36	35.8	4.42	0.14	4.28
ZnAlZr-LDH	93	0.62	27.4	4.83	0.19	4.64
Ru/ZnAl-LDH	57	0.54	32.3	4.61	0.17	4.44
Ru/ZnAlZr-LDH	119	0.26	6.5	5.02	0.23	4.79
Ru/ZnAlSn-LDH	128	0.31	6.2	5.10	0.24	4.86

[a] BET specific surface area.
[b] Total pore volume.
[c] Mean pore diameter.
[d] Weak base sites = total base sites-medium strength and strong base sites.

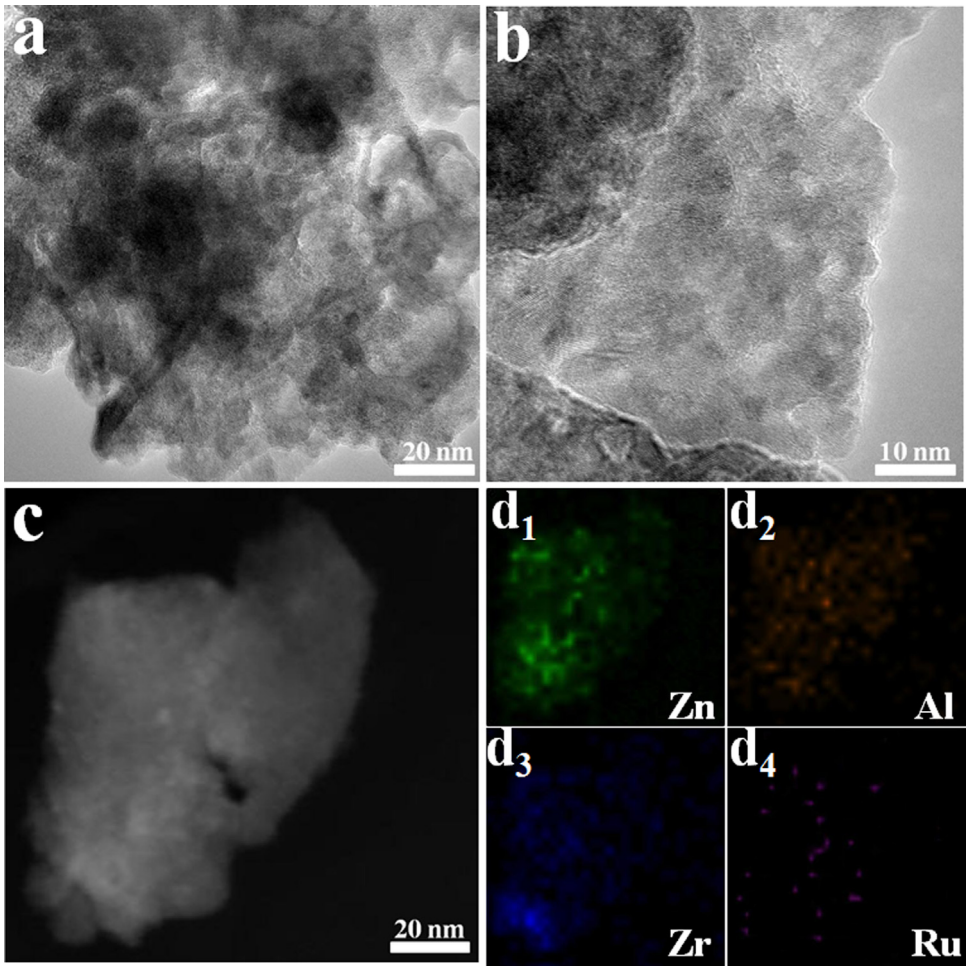

Fig. 2. HRTEM (a,b) and HAADF-STEM image (c) of representative Ru/ZnAlZr-LDH sample with the EDX mapping of Zn-K, Al-K, Zr-K and Ru-K (d).

ing of 0.9 wt% shows enhanced catalytic performance with a high EL conversion of 89% and a GVL selectivity of 94% (entry 7). Moreover, it is found that Ru^0/ZnAlZr-LDH sample exhibits a catalytic performance similar to that of ZnAlZr-LDH (entry 8), indicating that Ru^0 species are not catalytically active sites in the present catalytic reaction. Previously, it was reported that surface acid-base property of catalysts could significantly affect the activity and selectivity in the transfer hydrogenation of carbonyl compounds [32]. As for LDH materials, surface acidity mainly originates from metal cations, which are considered as Lewis acidic sites. In order to identify the effect of surface acid-base property on the catalytic performance, Ru/ZnAlSn-LDH sample also was synthesized. Because the electronegativity of Sn^{4+} cation is almost equal to that of Zr^{4+} cation, it is expected that the strength and type of surface acidic sites should keep unchanged if Zr^{4+} ions in brucite-like layers are replaced by Sn^{4+} ions. Moreover, the total number of base sites on the Ru/ZnAlSn-LDH is slightly higher than that on the Ru/ZnAlZr-LDH (Table 1). However, the catalytic reaction result indicates that Ru/ZnAlSn-LDH exhibits a less activity than Ru/ZnAlZr-LDH in spite of a similar GVL selectivity (entry 9).

In addition, when the dosage of Ru/ZnAlZr-LDH is increased from 0.1 g to 0.2 g, the EL conversion and the GVL selectivity reach 94% and 95% after reaction for a very short time of 10 min, respectively (entry 10), due to the increased amount of active sites. If the Ru loading is decreased from 0.9 wt% to 0.6 wt%, both the EL conversion and the GVL selectivity over the Ru/ZnAlZr-LDH are slightly reduced to 90% and 92%, respectively, after 10 min (entry 11). It demonstrates that surface catalytically active sites should be highly dispersed on the Ru/ZnAlZr-LDH in two cases of the Ru loadings of 0.6 and 0.9 wt%. If the amount of EL charged is decreased from 2.8 mmol to 1.4 mmol, an extremely high GVL yield of 98% can be achieved over the Ru/ZnAlZr-LDH with the Ru loading of 0.9 wt% after 10 min (entry 12).

Since Ru-containing catalysts show much higher catalytic performances than corresponding Ru-free LDH samples and Ru/ZnAlSn-LDH that has almost the same quantity of surface basic sites as Ru/ZnAlZr-LDH (Table 1), we speculate that the enhanced reaction activity of Ru/ZnAlZr-LDH may be correlated with the favorable electronic structure of Ru species. Further, noticeably, several reference samples, Au/ZnAlZr-LDH, Pd/ZnAlZr-LDH, $Ru(OH)_3$/$Zr(OH)_4$ and mechanical mixed sample of $Ru(OH)_3$ and ZnAlZr-LDH, present much lower activity than Ru/ZnAlZr-LDH under similar reaction conditions (entries 13–16). It seems that the kinds of supported metals, the modes of the interaction of Ru species with supports, and the types of supports greatly impact on the catalytic activity.

From the above results, it is clearly indicated that Ru/ZnAlZr-LDH catalyst exhibits an excellent activity for the EL transfer hydrogenation to produce GVL, demonstrating that its much higher activity may be related to special interaction between Ru species and the ZnAlZr-LDH support. Moreover, to carry out a rigorous comparison of the activities of different catalysts, the mass specific activity (MSA) of catalysts was determined by normalizing the initial reaction rate to the total amount of catalyst without the effects of products or adverse reactions. As shown in Fig. 3, obviously, the MSA value for pure ZnAlZr-LDH is much lower than those for Ru-

Table 2
The catalytic results of the transfer hydrogenation of EL over different samples.

Entry	Catalysts	Time (min)	Temp. (°C)	Zr: EL (mol%)	Ru:EL (mol%)	Conv.[a] (%)	Select.[b] (%)	R_{GVL}[c] (μmol g^{-1} min^{-1})	Yield of acetone (%)
1	ZnAl-LDH	30	200	–	–	24	65	146	2.9
2	MgAl-LDH	30	200	–	–	20	63	118	2.7
3	NiAl-LDH	30	200	–	–	16	57	85	2.0
4	CoAl-LDH	30	200	–	–	9	50	42	1.2
5	ZnAlZr-LDH	30	200	3.4	–	49	72	329	6.3
6	Ru/ZnAl-LDH	30	200	–	0.3	78	90	655	10.1
7	Ru/ZnAlZr-LDH	30	200	3.5	0.3	89	94	781	11.8
8	Ru^0/ZnAlZr-LDH	30	200	3.5	0.3	51	71	338	6.5
9	Ru/ZnAlSn-LDH	30	200	–	0.3	81	93	703	10.4
10	Ru/ZnAlZr-LDH[d]	10	200	7.0	0.6	94	95	1250	12.5
11	Ru/ZnAlZr-LDH[e]	10	200	7.0	0.4	90	92	1163	12.0
12	Ru/ZnAlZr-LDH[f]	10	200	14.0	1.2	100	98	686	13.8
13	Au/ZnAlZr-LDH[d]	10	200	7.0	–	42	81	476	5.7
14	Pd/ZnAlZr-LDH[d]	10	200	7.0	–	44	96	591	5.8
15	$Ru(OH)_3/Zr(OH)_4$[d]	10	200	7.0	0.6	63	90	794	8.5
16	$Ru(OH)_3$-ZnAlZr-LDH[g]	30	200	3.4	0.3	54	76	383	7.3
17	Zr-HBA[h]	60	200	88.1	–	100	97	81	–
18	$Zr(OH)_4$[i]	60	200	45.3	–	94	95	207	–
19	$Ru(OH)_x/TiO_2$[j]	1440	90	–	4.2	100	88	6	–
20	Zr-MOFs[k]	180	130	18.0	–	100	85.0	94	–
21	Raney Ni[l]	540	80	–	–	100	100	62	–
22	Cu-Ni/Al_2O_3[m]	720	150	–	–	100	97	14	–

[a] Reaction conditions: reaction temperature, 200 °C; catalyst, 0.1 g; EL, 2.8 mmol; isopropanol, 131 mmol; N_2 atmosphere.
[b] Major by-product was isopropyl levulinate.
[c] GVL formation rate.
[d] Catalyst, 0.2 g.
[e] Catalyst with the Ru loading of 0.6 wt%, 0.2 g.
[f] Catalyst with the Ru loading of 0.9 wt%, 0.2 g; EL, 1.4 mmo.
[g] Mechanical mixture of $Ru(OH)_3$ and ZnAlZr-LDH; the amount of Ru, 0.9 wt%.
[h] The data from ref. [33].
[i] The data from ref. [30]; catalyst, 0.2 g; EL, 1 mmol; isopropanol 100 mmol.
[j] The data from ref. [31].
[k] The data from ref. [48].
[l] The data from ref. [49].
[m] The data from ref. [50].

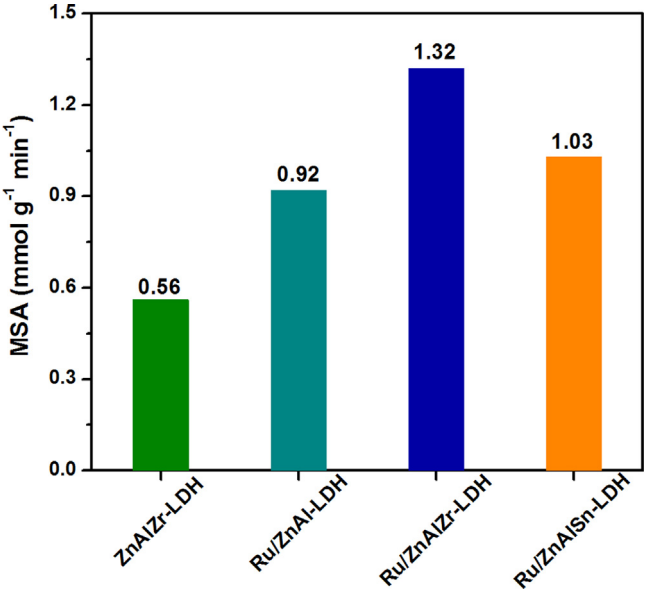

Fig. 3. Comparison of MSA values over different catalysts. Reaction conditions: reaction temperature, 200 °C; catalyst, 0.1 g; EL, 2.8 mmol; isopropanol, 131 mmol; N_2 atmosphere; Ru loading: 0.9 wt%.

containing catalysts. Among them, Ru/ZnAlZr-LDH possesses the highest MSA value (1.32 mmol g^{-1} min^{-1}). It means that the high activity of ZnAlZr-LDH alone seems unlikely. The improved transfer hydrogenation activity of Ru/ZnAlZr-LDH should be attributed to the introduction of highly dispersed Ru species on the surface of ZnAlZr-LDH. Despite different reaction conditions, the attained

Table 3
Catalytic hydrogenation performance over Ru/ZnAlZr-LDH catalyst.[a]

Hydrogen donors	Conv. (%)	Select. To GVL (%)	Yield of GVL (%)
ethanol	52	92	48
1-butanol	34	92	31
2-butanol	100	93	93
cyclohexanol	62	93	58

[a] Conditions: Ru/ZnAlZr-LDH, 0.2 g; EL, 2.8 mmol; solvent, 131 mmol; reaction time, 10 min; reaction temperature, 200 °C; N_2 atmosphere.

GVL formation rate over the Ru/ZnAlZr-LDH, which is calculated based on the moles of GVL produced to the total amount of catalyst within the entire reaction time period (Table 2), is about 15.4, 6.0, 13.3, and 208 times as those over Zr-HBA [33], $Zr(OH)_4$ [30], Zr-MOFs [48] and $Ru(OH)_x/TiO_2$ [31] previously reported, respectively, although there are much lower Zr or Ru contents in the Ru/ZnAlZr-LDH (Table 2). Furthermore, the GVL formation rate of Ru/ZnAlZr-LDH is also much higher than those of Raney Ni and Cu-Ni/Al_2O_3 catalysts reported previously [49,50]. The results strongly confirm the much higher intrinsic activity of the present Ru/ZnAlZr-LDH. As shown in Fig. 4, the GVL yield over the Ru/ZnAlZr-LDH reaches the maximum (about 97%) after a reaction time of 50 min. It demonstrates that 50 min is the optimum reaction time under the present reaction conditions (i.e. catalyst, 0.1 g; 200 °C; EL, 2.8 mmol; isopropanol, 131 mmol).

Different hydrogen donors including primary alcohols (ethanol and 1-butanol) and secondary alcohols (2-butanol and cyclohexanol) also were examined in the transfer hydrogenation of EL (Table 3). Noticeably, in the presence of 2-butanol, Ru/ZnAlZr-LDH yields a complete EL conversion. In contrast, a much lower EL conversion of 34% is obtained in the case of 1-butanol. Regardless different EL conversions, the GVL selectivity remains almost

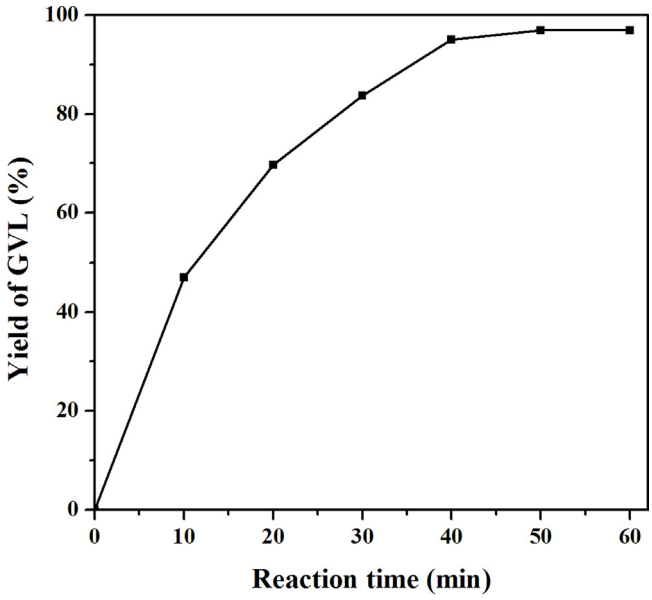

Fig. 4. Yield of GVL over the Ru/ZnAlZr-LDH as a function of reaction time in the transfer hydrogenation of EL. Reaction conditions: reaction temperature, 200 °C; catalyst, 0.1 g; EL, 2.8 mmol; isopropanol, 131 mmol; N_2 atmosphere.

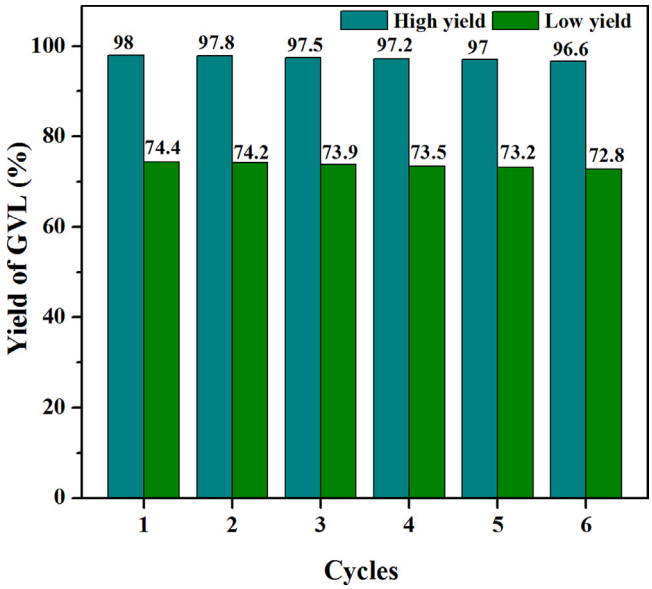

Fig. 5. Recycling property of Ru/ZnAlZr-LDH catalyst. Conditions: catalyst, 0.2 g; 200 °C; 10 min; isopropanol, 131 mmol; EL, 1.4 mmol (high yield level) or 2.8 mmol (low yield level); N_2 atmosphere.

unchanged in all cases. This suggests that the nature of hydrogen donors cannot affect the selectivity in the present catalytic systems.

Fig. 5 show the stability of the Ru/ZnAlZr-LDH catalyst determined by six consecutive catalytic tests at two different EL conversion levels. After each recycling experiment, the used catalyst was separated by filtration, dried at 70 °C for 12 h, and reused in the next reaction. It is noted that no obvious decline in GVL yields is observed at two different conversion levels after it is reused for six successive recycling runs. Possible Ru leaching was also investigated by ICP-AES and the results reveal that the leaching of ruthenium in the solution after six consecutive cycles is negligible. The above results indicate the excellent stability and reusability of the Ru/ZnAlZr-LDH catalyst, owing to the strong interactions between Ru species and the ZnAlZr-LDH matrix. To date, the present Ru-based catalyst exhibited an unprecedented high performance in the transfer hydrogenation of EL, with respect to other Zr- or Ru-based catalysts previously reported.

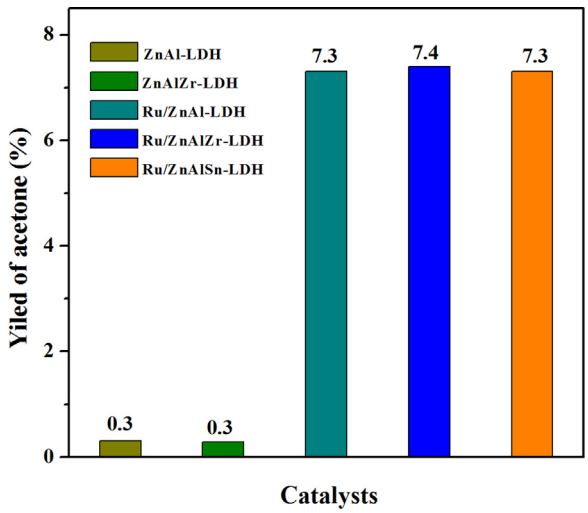

Fig. 6. Change in the yield of acetone with different samples. Conditions: catalyst, 0.2 g; isopropanol, 131 mmol; 2 h; 200 °C; N_2 atmosphere.

3.3. Catalytic reaction mechanism

In the present transfer hydrogenation process, easy dehydrogenation of the hydroxyl group in isopropanol can greatly facilitate the hydrogenation of EL to generate GVL. In order to find out the origin of catalytic performance, the dehydrogenation ability of different samples was investigated. As shown in Fig. 6, in the absence of EL substrate, the yields of acetone obtained over ZnAl-LDH and ZnAlZr-LDH are much lower than those over Ru/ZnAl-LDH, Ru/ZnAlZr-LDH and Ru/ZnAlSn-LDH, strongly mirroring that the dehydrogenation ability of Ru-free samples are lower than that of Ru-containing samples. Moreover, Ru/ZnAl-LDH, Ru/ZnAlZr-LDH and Ru/ZnAlSn-LDH almost deliver an identical yield of acetone, demonstrating that the partial replacement of Al to Zr or Sn does not contribute to the dehydrogenation of isopropanol in the present catalytic systems. Previously, however, it was reported that the conversion of isopropanol to acetone/hydrogen could not be observed in the absence of EL [51]. Our result further demonstrates that the existence of Ru species in the Ru/ZnAlZr-LDH is highly beneficial to the dehydrogenation of isopropanol, thus enhancing catalytic activity of the catalyst.

Commonly, surface basicity of catalysts is good for the transfer hydrogenations [40,52], because dehydrogenation process can proceed through the abstraction of the hydrogen in isopropanol on basic sites. The method based on irreversible adsorption of organic acids including acrylic acid and phenol has been used to determine the amount of surface basic sites of uncalcined LDH materials. As shown in Table 1, the number of total basic sites in the Ru/ZnAl-LDH (4.61 mmol acrylic acid/g) is slightly higher than that in the ZnAl-LDH (4.42 mmol acrylic acid/g), probably due to the fact that only basic sites on the external surface of the catalyst can be absorbed. Similarly, ZnAlZr-LDH sample containing Zr in the brucite-like layers has a larger number of surface basic sites in comparison to ZnAl-LDH, due to higher surface area of ZnAlZr-LDH. It demonstrates that high surface area of LDH materials facilitates the exposure of surface hydroxyl groups on the brucite-like layers. Moreover, all the samples possess a small quantity of surface medium-strength and strong basic sites. However, among all samples, the change in the number of basic site is much smaller than that of the specific surface area. Meanwhile, in situ FT-IR spectra

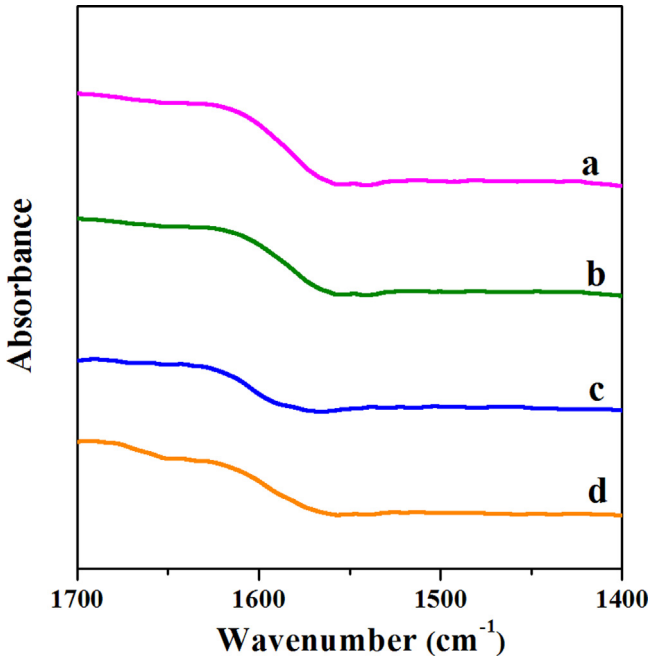

Fig. 7. In situ FT-IR spectra (B) of pyridine adsorbed on different samples: (a) ZnAl-LDH, (b) Ru/ZnAl-LDH, (c) Ru/ZnAlZr-LDH and (d) Ru/ZnAlSn-LDH.

of pyridine adsorbed on different samples were measured (Fig. 7) reveal that no obvious vibration bands at about 1454 cm^{-1} and 1540 cm^{-1} related to surface Lewis and Brønsted acidic sites are observed in each case, indicative of the lack of surface acidity. The above results reflect that surface acid-base property of present LDH-based catalyst systems should not be responsible for the difference in their transfer hydrogenation performances.

Further, two poisoning experiments were carried out by introducing extra additives into the reaction system to gain more insight into the mechanism for the transfer hydrogenation of EL and the reaction results are shown in Table 4. In the presence of benzoic acid in the reaction system, the EL conversion is sharply decreased to 33%. The benzoic acid may react with isopropanol to generate ethers, thus restraining the conversion of EL. However, the molar ratio of benzoic acid to isopropanol is only 0.03. Therefore, the rapid decrease in the EL conversion should mainly be ascribed to the blocking of surface basic sites, indicating that the crucial role of surface hydroxyl groups on the lattice of Ru/ZnAlZr-LDH as basic sites in the present catalytic process. In addition, if pyridine is added into the reaction system to block surface acidic sites, the catalytic activity of Ru/ZnAlZr-LDH is slightly decreased. Previously, it was reported that surface Lewis acid sites could strongly improve the MPV hydride transfer reaction [40,53–55]. Conventionally, Zr and Sn oxides are considered as strong Lewis acid solids. However, our above results clearly demonstrate that in the case of Ru/ZnAlZr-LDH, Zr^{4+} species should be located within the brucite-like layers through substituting Al^{3+} ions in the LDH. Thus, such Zr^{4+} species is not suitable to provide Lewis acid sites, and surface acidity of Ru/ZnAlZr-LDH catalyst is not a main driving force in the present EL transfer hydrogenation.

Table 4
Effect of different additives on the transfer hydrogenation of EL over the Ru/ZnAlZr-LDH.[a]

Additives	Conv. (%)	Select. to GVL (%)
benzoic acid	33	85
pyridine	89	92

[a] Conditions: 200 °C; 10 min; isopropanol, 131 mmol; EL, 2.8 mmol; catalyst, 0.2 g; N_2 atmosphere; additive, 0.5 g.

On the other side, it is well-known that the electronic property of active metal centers in catalysts plays a crucial role for a broad range of heterogeneous reactions. In particular, in the case of the hydrogenation process of carbonyl-containing compounds, the backbonding of d electrons of electron-rich metal sites to π orbitals of the carbonyl group can improve the adsorption and the activation of the C=O bond [56]. In order to obtain the basic clues concerning the interaction between Ru species and different LDH matrixes, XPS characterization of Ru-containing samples was performed. As shown in Fig. 8, clearly, the binding energy (BE) value of Ru species increases gradually from 281.4 eV for Ru/ZnAlZr-LDH to 281.7 eV for Ru/ZnAlSn-LDH and 282.0 eV for Ru/ZnAl-LDH, reflecting that Ru species exist in the form of $Ru(OH)_3$ in all samples [57,58]. Especially, a larger amount of electron-rich Ru^{3+} species can form in the Ru/ZnAlZr-LDH. Such electron-rich state of Ru species with the increased electron cloud density should be correlated with the presence of strong interaction between Ru^{3+} species and the ZnAlZr-LDH matrix. Interestingly, we also observe a negative correlation between the activity of catalysts and the BE values of Ru^{3+} species. The lower the BE value, the higher the activity. Ru/ZnAlZr-LDH with a lowest BE value exhibits a highest activity. The kind of electron-rich Ru^{3+} species probably facilitate π-back bonding to

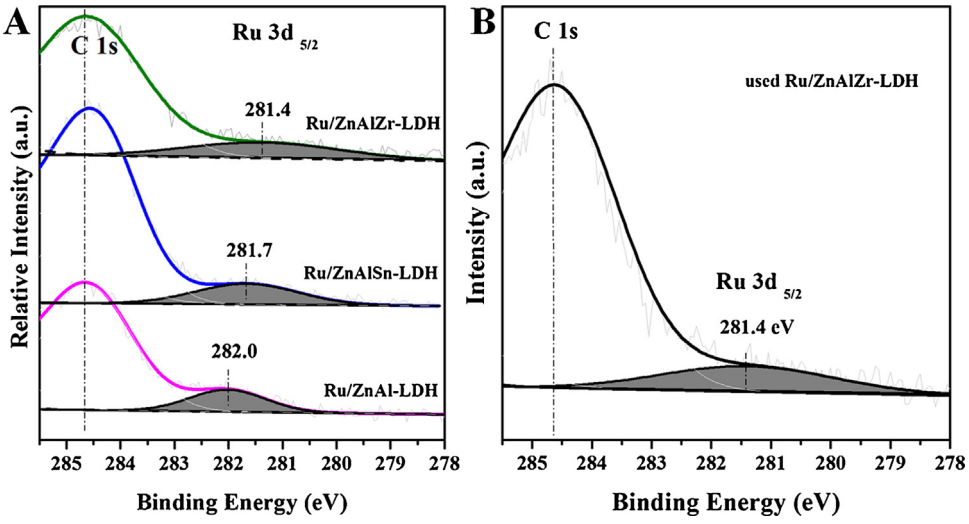

Fig. 8. XPS of Ru 3d region for different supported Ru-containing samples (A) and used Ru/ZnAlZr-LDH (B) after reaction.

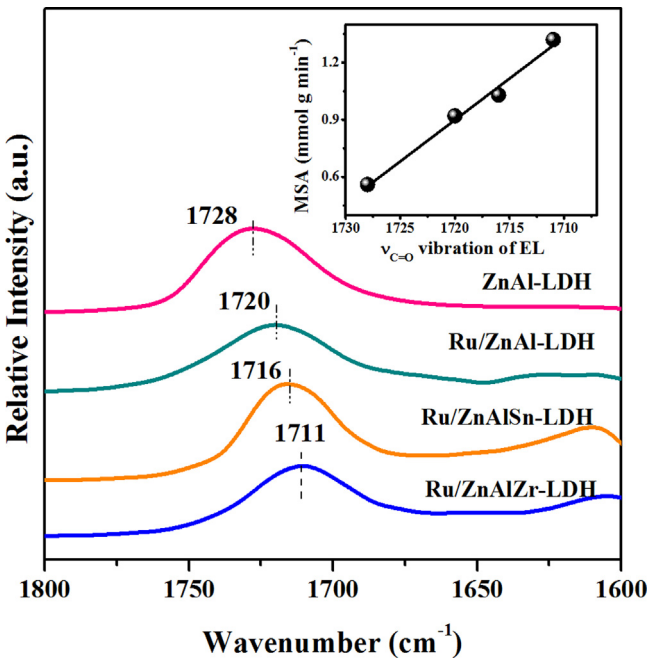

Fig. 9. In situ FT-IR spectra of EL adsorbed on different catalysts. The Inset shows the correlation between IR band positions of EL adsorbed on catalysts and MSA values for transfer hydrogenation of EL by different catalysts.

the carbonyl group in EL and thus the adsorption and activation of the C=O bond. Further, the XPS result of recovered Ru/ZnAlZr-LDH shows that the binding energy of Ru species for 3d 5/2 core level still is about 281.4 eV. It demonstrates that Ru^{3+} species in the catalyst cannot be reduced to metallic Ru^0 species by isopropanol or in situ formed active hydrogen species during reaction process.

Further, to understand the origin of the unparalleled catalytic activity of Ru/ZnAlZr-LDH catalyst in the transfer hydrogenation of EL, the interaction between the catalyst surface and C=O group in EL was studied by in situ FT-IR spectra of EL adsorbed on different samples at room temperature (Fig. 9). For ZnAl-LDH sample, the adsorption at 1728 cm^{-1} is assigned to the stretching vibration of the C=O bond in adsorbed EL [59]. Noticeably, the wavenumber for the stretching vibration of the C=O bond decreases progressively in the order of ZnAl-LDH > Ru/ZnAl-LDH > Ru/ZnAlSn-LDH > Ru/ZnAlZr-LDH, reflecting that Ru/ZnAlZr-LDH interacts more strongly with carbonyl group of the EL than other samples. Therefore, the introduction of simultaneous Ru and Zr species into the catalyst is greatly beneficial to the activation of the C=O bond. This may be mainly assigned to the electron-rich state of Ru species in the Ru/ZnAlZr-LDH, which promotes the electron transfer from the Ru d orbital to the C=O $2\pi^*$ anti-bonding orbital, resulting in the weakness of the C=O bond strength. To quantitatively discuss the effect of the interaction between the catalyst surface and EL, a correlation between the positions of C=O bands (IR results) and the MSA value for transfer hydrogenation of EL by different catalysts is presented in the inset in Fig. 9. Notably, the MSA value linearly increases with the decrease in the wavenumber of C=O stretching band for EL adsorbed on catalysts. The above results demonstrate that the C=O bond of EL coordinated to electron-rich state of Ru species has lower the bond order and thus Ru/ZnAlZr-LDH catalyst exhibits the higher reactivity toward the EL hydrogenation.

Based on above characterizations and experimental results, a plausible mechanism for the transfer hydrogenation of EL to GVL over the Ru/ZnAlZr-LDH catalyst is tentatively proposed (Scheme 1). In general, the transfer hydrogenation of EL proceeds through two reaction routes: the one follows MPV reduction pathway involving an activated six member ring transition state related to surface hydroxyl groups [38,60], and the other one obeys a metal hydride route related to surface highly dispersive Ru species [61].

For MPV reaction route, firstly, isopropanol is adsorbed on surface hydroxyl groups on the LDH matrix and further dissociated to the corresponding alkoxide 1. Secondly, EL molecule coordinates with the alkoxide to form a six-membered ring transition state 2. Thirdly, the hydride from the alkoxide is transferred to the carbonyl in EL via a pericyclic mechanism. Subsequently, the new carbonyl dissociates and gives the intermediate species 3, while acetone is released. Fourthly, the intermolecular ligand exchange between intermediate species 3 and another isopropanol from solution leads to the generation of ethyl 4-hydroxypentanoate (4-HPE) and alkoxide 1. Finally, 4-PHE formed in this reaction system is rapidly converted to GVL through an intramolecular transesterification.

In the case of metal hydride route, firstly, ruthenium alkoxide species 1′ is formed via the ligand exchange occurring between surface ruthenium hydroxide and isopropanol. Then, β-hydride elimination occurs in species 1′, and ruthenium hydride species 2′ and acetone are formed. Subsequently, the reaction between species 2′ and EL substrate results in the formation of ketone–hydride species 3′. The hydride transfer from ruthenium hydride to the carbonyl carbon of EL in species 3′ gives other alkoxide species 4′. At last, similar to the MPV route, GVL can be produced through the intermolecular ligand exchange between alkoxide species 4′ and isopropanol and following intramolecular transesterification process.

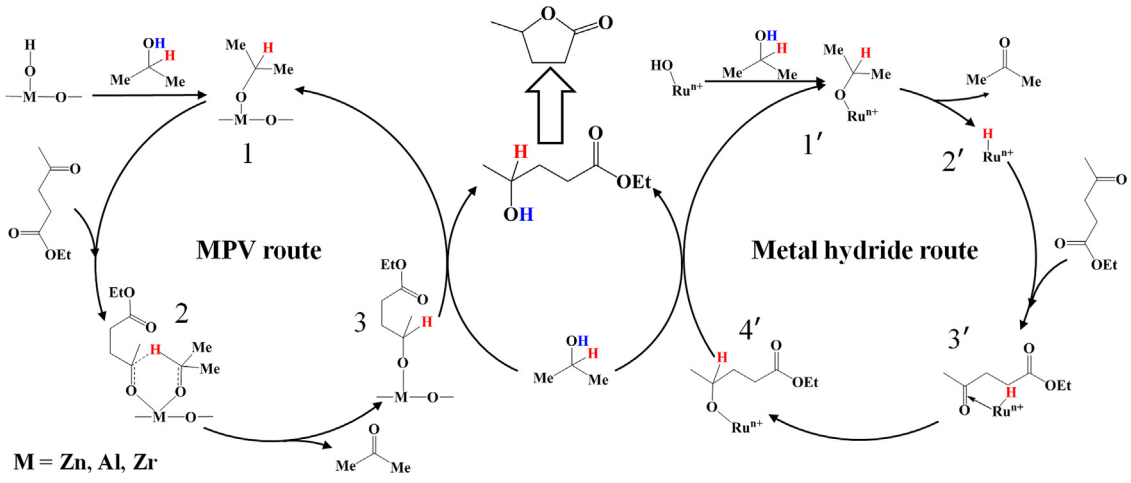

Scheme 1. Proposed possible mechanisms for the transfer hydrogenation of EL to GVL over the Ru/ZnAlZr-LDH.

Table 5
Transfer hydrogenation of different carbonyl compounds over the Ru/ZnAlZr-LDH catalyst.[a]

Entry	Substrates	Products	Conversion (%)	Selectivity (%)
1	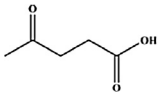	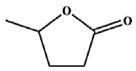	100	90
2	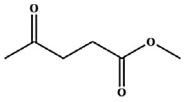	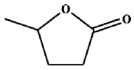	100	92
3	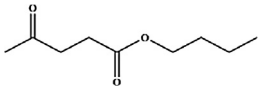	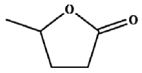	100	93
4	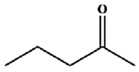	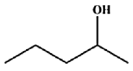	100	96
5	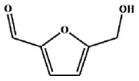	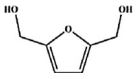	100	94
6	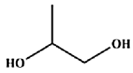	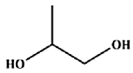	100	97
7	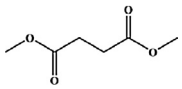	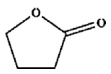	100	91

[a] Reaction conditions: 200 °C; 30 min; catalyst, 0.2 g; substrate, 2.8 mmol; isopropanol, 131 mmol; N_2 atmosphere.

As evidenced by poisoning experiments shown in Table 4, surface basic sites are highly essential for the high catalytic activity of catalysts. Moreover, the fact that the catalytic performance of Ru/ZnAlZr-LDH is much higher than that of ZnAlZr-LDH demonstrates that Ru^{3+} species also plays a key role in enhancing the catalytic activity. Surface basic sites and Ru^{3+} species, which are responsible for MPV reduction pathway and metal hydride route, respectively, are equally important for the present reaction. Therefore, two reaction routes have an equal status. In the present catalytic system, Ru/ZnAlZr-LDH provides both favorable electron-rich Ru^{3+} species and abundant hydroxyl groups on the catalyst surface, which can construct the most effective cooperative effect between them. As a result, the above proposed reaction mechanisms of catalytic transfer hydrogenation of EL reasonably explain the excellent catalytic performance of Ru/ZnAlZr-LDH catalyst.

3.4. Feasibility of the Ru/ZnAlZr-LDH catalyst

To verify the catalytic transfer hydrogenation ability of as-synthesized Ru/ZnAlZr-LDH catalyst, the feasibility of Ru/ZnAlZr-LDH was tested using several biomass-derived carbonyl compounds as substrates. As shown in Table 5, Notably, Ru/ZnAlZr-LDH can significantly catalyze these aldehydes and ketones to corresponding alcohols with high conversions (100%) and high selectivities to target alcohol products (90–97%) within a very short time of 10 min. Therefore, Ru/ZnAlZr-LDH shows great potential as an effective and versatile catalyst for the transfer hydrogenation of carbonyl compounds in terms of its excellent reactivity, reusability and feasibility.

4. Conclusions

In summary, we develop a new Ru/ZnAlZr-LDH catalyst with an unparalleled activity in the transfer hydrogenation of EL to GVL. By combination of Ru species with the ZnAlZr-LDH matrix, the electronic structure of Ru^{3+} species is relationally modified. XPS analysis confirms the electron-rich nature of Ru^{3+} species in the form of $Ru(OH)_3$. Ru/ZnAlZr-LDH catalyst presents an unprecedented activity with a high GVL yield of 98% only after reaction for 10 min, and yields a fastest GVL formation rate of 1250 $\mu mol\ g_{cat}^{-1}\ min^{-1}$ to date, with respect to other Zr- or Ru-based catalysts previously reported. Such unprecedented high performance of Ru/ZnAlZr-LDH can be attributable to a cooperative effect between double-active sites on the catalyst, e.g. a large amount of surface hydroxyl groups and highly dispersive electron-rich Ru species, which is beneficial to the activation of the hydroxyl group in isopropanol and the C=O bond in EL, thereby greatly facilitating the formation of activated six-membered ring transition state and active ruthenium-hydride species in the course of transfer hydrogenation processes. Moreover, as-synthesized Ru/ZnAlZr-LDH catalyst can be reused at least six times without obvious lose in the activity. The present readily available, highly efficient and stable ruthenium-based catalyst possesses promising potential for the practical production of commercially important chemicals from biomass-derived carbonyl compounds in terms of economic and environmental sustainability.

Acknowledgments

We gratefully thank the financial support from National Natural Science Foundation of China and the Fundamental Research Funds for the Central Universities (buctrc201528).

References

[1] C.O. Tuck, E. Pérez, I.T. Horváth, R.A. Sheldon, P.M. Oliakoff, Science 337 (2012) 695–699.
[2] M. He, Y. Sun, B. Han, Angew. Chem. Int. Ed. 52 (2013) 9620–9633.
[3] Y. Wang, Y. Miao, S. Li, L. Gao, G. Xiao, Mol. Catal. 436 (2017) 128–137.

[4] Q. Li, P. Man, L. Yuan, P. Zhang, Y. Li, S. Ai, Mol. Catal. 431 (2017) 32–38.
[5] J. Jae, W. Zheng, R.F. Lobo, D.G. Vlachos, ChemSusChem 6 (2013) 1158–1162.
[6] G.-H. Wang, J. Hilgert, F.H. Richter, F. Wang, H.-J. Bongard, B. Spliethoff, C. Weidenthaler, F. Schüth, Nat. Mater. 13 (2014) 293–300.
[7] J. Mitral, X. Zhou, T. Rauchfuss, Green Chem. 17 (2015) 307–313.
[8] H. Luo, D.F. Consoli, W.R. Gunther, Y. Román-Leshkov, J. Catal. 320 (2014) 198–207.
[9] Y. Yang, G. Gao, X. Zhang, F. Li, ACS Catal. 4 (2014) 1419–1425.
[10] S. Zhu, Y. Xue, J. Guo, Y. Cen, J. Wang, W. Fan, ACS Catal. 6 (2016) 2035–2042.
[11] O.A. Abdelrahman, A. Heyden, J.Q. Bond, ACS Catal. 4 (2014) 1171–1181.
[12] V. Mohan, V. Venkateshwarlu, C.V. Pramod, B.D. Raju, K.S.R. Rao, Catal. Sci. Technol. 4 (2014) 1253–1258.
[13] D.M. Alonso, S.G. Wettstein, J.A. Dumesic, Green Chem. 15 (2013) 584–595.
[14] D. Sun, A. Ohkubo, K. Asami, T. Katori, Y. Yamada, S. Sato, Mol. Catal. 437 (2017) 105–113.
[15] M. Al-Naji, A. Yepez, A.M. Balu, A.A. Romero, Z. Chen, N. Wilde, H. Li, K. Shih, R. Gläser, R. Luqueb, J. Mol. Catal. A: Chem. 417 (2016) 145–152.
[16] I.T. Horvath, H. Mehdi, V. Fabos, L. Boda, L.T. Mika, Green Chem. 10 (2008) 238–242.
[17] Z.-Q. Duan, F. Hu, Green Chem. 14 (2012) 1581–1583.
[18] E.I. Gurbuz, J.M.R. Gallo, D.M. Alonso, S.G. Wettstein, W.Y. Lim, J.A. Dumesic, Angew. Chem. Int. Ed. 52 (2013) 1270–1274.
[19] S.G. Wettstein, D.M. Alonso, Y. Chong, J.A. Dumesic, Energy Environ. Sci. 5 (2012) 8199–8203.
[20] H. Heeres, R. Handana, D. Chunai, C.B. Rasrendra, B. Girisuta, H.J. Heeres, Green Chem. 11 (2009) 1247–1255.
[21] J.Q. Bond, D. Wang, D.M. Alonso, J.A. Dumesic, J. Catal. 281 (2011) 290–299.
[22] D.M. Alonso, J.Q. Bond, J.C. Serrano-Ruiz, J.A. Dumesic, Green Chem. 12 (2010) 992–999.
[23] J.Q. Bond, D.M. Alonso, D. Wang, R.M. West, J.A. Dumesic, Science 327 (2010) 1110–1114.
[24] J.-P. Lange, R. Price, P.M. Ayoub, J. Louis, L. Petrus, L. Clarke, H. Gosselink, Angew. Chem. Int. Ed. 49 (2010) 4479–4483.
[25] C. Chang, G. Xu, X. Jiang, Bioresour. Technol. 121 (2012) 93–99.
[26] L. Peng, L. Lin, H. Li, Ind. Crops Prod. 40 (2012) 136–144.
[27] X. Du, L. He, S. Zhao, Y. Liu, Y. Cao, H. He, K. Fan, Angew. Chem. Int. Ed. 123 (2011) 7961–7965.
[28] L. Deng, J. Li, D.-M. Lai, Y. Fu, Q.-X. Guo, Angew. Chem. Int. Ed. 48 (2009) 6529–6532.
[29] J. Wang, S. Jaenicke, G.-K. Chuah, RSC Adv. 4 (2014) 13481–13489.
[30] X. Tang, H. Chen, L. Hu, W. Hao, Y. Sun, X. Zeng, L. Lin, S. Liu, Appl. Catal. B: Environ. 147 (2014) 827–834.
[31] Y. Kuwahara, W. Kaburagi, T. Fujitani, RSC Adv. 4 (2014) 45848–45855.
[32] M. Chia, J.A. Dumesic, Chem. Commun. 47 (2011) 12233–12235.
[33] J. Song, L. Wu, B. Zhou, H. Zhou, H. Fan, Y. Yang, Q. Meng, B. Han, Green Chem. 17 (2015) 1626–1632.
[34] Z. Yang, Y.-B. Huang, Q.-X. Guo, Y. Fu, Chem. Commun. 49 (2013) 5328–5330.
[35] F. Li, X. Duan, Struct. Bonding. 119 (2006) 193–223.
[36] G. Fan, F. Li, D.G. Evans, X. Duan, Chem. Soc. Rev. 43 (2014) 7040–7066.
[37] P.J. Sideris, U.G. Nielsen, Z. Gan, C.P. Grey, Science 321 (2008) 113–117.
[38] W. Hao, W. Li, X. Tang, X. Zeng, Y. Sun, S. Liu, L. Lin, Green Chem. 18 (2016) 1080–1088.
[39] M.J. Climent, A. Corma, S. Iborra, K. Epping, A. Velty, J. Catal. 225 (2004) 316–326.
[40] M. Shirotori, S. Nishimura, K. Ebitani, Catal. Sci. Technol. 4 (2014) 971–978.
[41] E. Li, Z.P. Xu, V. Rudolph, Appl. Catal. B: Environ. 88 (2009) 42–49.
[42] M. Shirotori, S. Nishimura, K. Ebitani, Catal. Sci. Technol. 6 (2016) 8200–8211.
[43] Q. Hu, G. Fan, F. Li, J. Catal. 340 (2016) 184–195.
[44] R. Ionescu, O.D. Pavel, R. Bîrjega, R. Zăvoianu, E. Angelescu, Catal. Lett. 134 (2010) 309–317.
[45] O.D. Pavel, R. Zăvoianu, R. Bîrjega, E. Angelescu, Catal. Commun. 12 (2011) 845–850.
[46] S. Sankaranarayanan, A. Sharma, K. Srinivasan, Catal. Sci. Technol. 5 (2015) 1187–1197.
[47] C. Rudolf, B. Dragoi, A. Ungureanu, A. Chirieac, S. Royer, A. Nastro, E. Dumitriu, Catal. Sci. Technol. 4 (2014) 179–189.
[48] A.H. Valekar, K.-H. Cho, S.K. Chitale, D.-Y. Hong, G.-Y. Cha, U.-H. Lee, D.W. Hwang, C. Serre, J.-S. Chang, Y.K. Hwang, Green Chem. 18 (2016) 4542–4552.
[49] Z. Yang, Y.-B. Huang, Q.-X. Guo, Y. Fu, Chem. Commun. 49 (2013) 5328–5330.
[50] B. Cai, X.-C. Zhou, Y.-C. Miao, J.-Y. Luo, H. Pan, Y.-B. Huang, ACS Sustainable Chem. Eng. 5 (2017) 1322–1331.
[51] Z. Xue, J. Jiang, G. Li, W. Zhao, J. Wang, T. Mu, Catal. Sci. Technol. 6 (2016) 5374–5379.
[52] Q. Hu, G. Fan, L. Yang, X. Cao, P. Zhang, B. Wang, F. Li, Green Chem. 18 (2016) 2317–2322.
[53] L. Bui, H. Luo, W.R. Gunther, Y. Román-Leshkov, Angew. Chem. Int. Ed. 52 (2013) 8022–8025.
[54] Y. Zhu, G. Chuah, S. Jaenicke, J. Catal. 227 (2004) 1–10.
[55] C. Jiménez-Sanchidrián, J.M. Hidalgo, J.R. Ruiz, Appl. Catal. A: Gen. 303 (2006) 23–28.
[56] Y.-K. Lee, S.T. Oyam, J. Catal. 239 (2006) 376–389.
[57] M. Matsushita, K. Kamata, K. Yamaguchi, N. Mizuno, J. Am. Chem. Soc. 127 (2005) 6632–6640.
[58] M. Kotani, T. Koike, K. Yamaguchi, N. Mizuno, Green Chem. 8 (2006) 735–741.
[59] J.M. Tukacs, D. Király, A. Strádi, G. Novodarszki, Z. Eke, G. Dibó, T. Kégl, L.T. Mika, Green Chem. 14 (2012) 2057–2065.
[60] R. Cohen, C.R. Graves, S.T. Nguyen, J.M.L. Martin, M.A. Ratner, J. Am. Chem. Soc. 126 (2004) 14796–14803.
[61] K. Yamaguchi, T. Koike, M. Kotani, M. Matsushita, S. Shinachi, N. Mizuno, J. Chem. Eur. 11 (2005) 6574–6582.